Ultrasonics Sonochemistry 83 (2022) 105926

Contents lists available at ScienceDirect

Ultrasonics Sonochemistry

journal homepage: www.elsevier.com/locate/ultson

Continuous production of nanoemulsion for skincare product using a 3D-printed rotor-stator hydrodynamic cavitation reactor

Nichagan Matman [a], Ye Min Oo [a], Thanaporn Amnuaikit [b], Krit Somnuk [a,c,*]

[a] Department of Mechanical and Mechatronics Engineering, Faculty of Engineering, Prince of Songkla University, Hat Yai, Songkhla 90110, Thailand
[b] Department of Pharmaceutical Technology, Faculty of Pharmaceutical Sciences, Prince of Songkla University, Hat Yai, Songkhla 90110, Thailand
[c] Energy Technology Research Center, Faculty of Engineering, Prince of Songkla University, Hat Yai, Songkhla 90110, Thailand

ARTICLE INFO

Keywords:
Hydrodynamic cavitation
Nanoemulsion
3D-printing technology
Niacin release profile

ABSTRACT

In this study, nanoemulsions for skincare products were continuously produced using a hydrodynamic cavitation reactor (HCR) designed with a rotor and stator. The key component of this research is the utilization of a 3D-printed rotor in a HCR for the production of an oil-in-water nanoemulsion. Response surface methodology was used to determine the process conditions, such as speed of the rotor, flow rate, as well as, Span60, Tween60, and mineral oil concentrations, for generating the optimal droplet size in the nanoemulsion. The results showed that a droplet size of 366.4 nm was achieved under the recommended conditions of rotor speed of 3500 rpm, flow rate of 3.3 L/h, Span60 concentration of 2.36 wt%, Tween60 concentration of 3.00 wt%, and mineral oil concentration of 1.76 wt%. Moreover, the important characteristics for consideration in skincare products, such as polydispersity index, pH, zeta potential, viscosity, stability, and niacin released from formulations, were also assessed. For the niacin release profile of emulsion and nanoemulsion formulations, different methods, such as magnetic stirring, ultrasound, and hydrodynamic cavitation, were compared. The nanoemulsion formulations provided a greater cumulative release from the formulation than the emulsion. Particularly, the nanoemulsion generated using the HCR provided the largest cumulative release from the formulation after 12 h. Therefore, the present study suggests that nanoemulsions can be created by means of hydrodynamic cavitation, which reduces the droplet size, as compared to that generated using other techniques. The satisfactory results of this study indicate that the rotor-stator-type HCR is a potentially cost-effective technology for nanoemulsion production.

1. Introduction

Nowadays, there is an increase in the number of people with skin issues such as skin inflammation, skin disorders such as eczema, psoriasis, hives, and ichthyosis, sunburn, acne, skin dryness, and other skin illnesses, amongst other conditions [1]. People with dermatitis, dry, oily, or sensitive skin can consult a dermatologist and easily procure cosmetics for their skin types at any beauty shop, to treat their skin. There are also various types of widely used treatment products, such as creams, lotions, and gels, which come with adequate and safe instructions and recommendations [2]. Therefore, cosmetics are becoming essential daily products for everyone, including men, women, and children. The coronavirus disease 2019 (COVID-19) outbreak is currently affecting people worldwide. In the pandemic, people, especially public health workers, must wash their hands more frequently with alcohol-based hand sanitizers and soaps, to prevent the spread of COVID-19 [3]. These alcohol-based hand sanitizers cause cracked or dry skin due to the loss of moisture content from the skin [4].

Emulsion lotion or cream is commonly used to prevent the skin from drying out as it helps in retaining moisture. The ingredients in the emulsion, such as mineral oil, glycerin, sorbitol, and isopropyl myristate, can assist in restoring the essential hydration of the skin. High-quality moisturizing creams, lotions, and gels contain the cosmetic ingredients of elastin, collagen, and glycosaminoglycans, which help restore moisture and prevent skin drying and aging. Owing to their properties, these help maintain skin hydration when applied throughout the day [5]. Therefore, there is no doubt that the global cosmetics market continues to grow annually. The Global Cosmetic Skin Care Market forecasted that the global market for cosmetic skincare demand was USD 185.5 billion in the year 2027, which was more than the

* Corresponding author at: Department of Mechanical and Mechatronics Engineering, Faculty of Engineering, Prince of Songkla University, Hat Yai, Songkhla 90110, Thailand.
E-mail address: krit.s@psu.ac.th (K. Somnuk).

https://doi.org/10.1016/j.ultsonch.2022.105926
Received 8 August 2021; Received in revised form 11 January 2022; Accepted 16 January 2022
Available online 20 January 2022

estimated amount of USD 145.3 billion by 2020 according to an analysis for the global cosmetic market in the period of 2020–2027 [6]. In the United States of America, the cosmetic skincare market is expected to be worth USD 39.2 billion by 2020. In Asia, China's cosmetic skincare industry is predicted to reach USD 38.9 billion in demand from 2020 to 2027, with a compound annual growth rate of 6.5%. In addition, other main markets, including Japan, Germany, and Canada, are projected to increase by approximately 1%, 1.8%, and 2.7%, respectively, from 2020 to 2027 [6].

This study focused on the production of skincare lotions, where viscosity is one of the most essential criteria in the emulsion formulation. Viscosity is also an essential factor when considering the type of cosmetic emulsion. Emulsion types are generally classified in terms of viscosity, with creams and gels having a higher viscosity, and lotions having a low to medium viscosity [7,8]. Anggelina *et al.* (2021) reported that viscosities greater than and less than 30000 cP are classified as creams and lotions, respectively [9,10]. The viscosity of the final product depends on the various ingredients in the emulsion formulation, mixing process, and storage time [8]. Furthermore, the degree of acidity and alkalinity (pH) are important parameters in cosmetic products. This is because the pH of cosmetics influences absorption and could induce irritation of the skin. Many researchers have studied the pH values for cosmetic products, which usually range between 5.0 and 8.0, depending on the ingredients used in the emulsion formulation [11].

The majority of oil emulsion lotions are made with oil-in-water (O/W) and water-in-oil (W/O) emulsions, which are used to combine two or more immiscible liquids into a homogenous liquid phase [12]. The key components of a lotion are the aqueous phase, oily phase, and emulsifying agents, such as Span60, Span80, Tween60, and Tween80. Surfactants are frequently used to prevent separation of these two phases [13]. Many other popular ingredients, including fragrances, glycerol, petroleum jelly, dyes, preservatives, and stabilizing agents, are normally mixed with lotions, to enhance their organoleptic and preservation characteristics [14]. The cosmetics and skincare industries are growing, especially for high-quality lotion production. Most formulated emulsions are designed to be quickly absorbed into the skin. Some desired features of emulsions include being a rich moisturizer with a light texture that does not thicken like a cream, and also being a light moisturizer.

There is a preference for emulsions that permeate through the human skin more rapidly and replenish the skin feeding more efficiently [15]. The human skin is composed of three layers: the epidermis, dermis, and hypodermis [16]. The epidermis is the outermost layer of the skin, which provides waterproof barriers and creates the skin tone. The dermis layer lies beneath the epidermis and consists of connective tissues, hair follicles, and sweat glands. The hypodermis layer is the deepest subcutaneous tissue, which is composed of fat and connective tissues [17,18]. Generally, upon applying lotion, emulsions can only permeate into the epidermis layer. The epidermis (also known as the stratum corneum) has the purpose of acting as a barrier to prevent external materials, such as bacteria, viruses, and other particles, from entering the body [19,20]. Therefore, lotions are developed specifically using various methods, to deliver some of its ingredients deeper than the epidermis, to the dermis layer. Microemulsions and nanoemulsions are specifically considered for this purpose, since their small droplet size boosts the permeability and delivery of the product to this layer by the skin [20]. Emulsions can be classified into three types, macroemulsions, nanoemulsions, and microemulsions. Macroemulsions are thermodynamically unstable, with droplet sizes ranging from 1000 to 10000 nm. This droplet size range of macroemulsions is the initial condition during the formation of nanoemulsions, and is subsequently converted into the droplet size range for nanoemulsions [21]. Nanoemulsions display low thermodynamical stability but are high kinetically stable, thereby preventing droplet size aggregation. The most frequently observed emulsions are O/W and W/O emulsions, which can be produced into droplet sizes ranging from 20 to 500 nm [22,23]. The droplet size of a microemulsion is typically between 10 and 100 nm. Microemulsions may develop spontaneously or with very low energy consumption. However, microemulsions require a greater quantity of surfactant for stabilization than nanoemulsions, which may have an impact on droplet size, toxicity, and irritation [21]. In contrast, surfactants are used in lower quantities in nanoemulsions. Other benefits of nanoemulsions include enhanced drug bioavailability, greater loading capacity for lipophilic active ingredients, non-toxicity, non-irritant systems, and the ability to transport active substances that can then directly be applied to the desired skin layer [24].

There are two methods for nanoemulsion preparation: high- and low-energy-consuming emulsification methods [25]. The low-energy emulsification method transports nano-sized emulsion droplets using the stored energy of the system, such as phase transition, self-emulsification, and phase inversion temperature. However, there are some advantages of the independent variables, such as the composition and temperature, which can affect the quality of the products in terms of the hydrophilic-lipophilic balance (HLB) of the formulations [12]. In the high-energy emulsification method, mechanical mixing with equipment such as a micro-fluidizer, a high-pressure homogenizer, and an ultrasonic sonicator, can create a homogeneous nanoemulsion by breaking down the water and oil phases under high pressures of 3.4 to 34.4 MPa [25]. Sharma *et al.* (2020) studied the high-shear mixing involved in microfluidization, in which the emulsion formulations are dosed into the microchannel mixer to obtain nanoemulsions under high-pressure in the range of 3.4–137.9 MPa [26]. Another interesting technique reported by Manickam *et al.*, 2020 involved a combination of ultrasound and microchannels to produce an O/W nanoemulsion [22]. In their study, pre-homogenization was performed using an ultrasonic horn, and the mixture was fed into different configurations of microchannels, which were fabricated with a silicon tube to enhance the characteristics of the nanoemulsion [22]. This method requires high energy and may only be suitable at the laboratory scale [27]. Jasmina *et al.* (2017) studied the ability of a high-pressure homogenizer to force the liquid through a narrow nozzle with high-pressure, from 3.4 to 34.4 MPa, to achieve an extremely low droplet size [25]. Ultrasound is another efficient method for nanoemulsion preparation, and high-intensity ultrasound is utilized to produce nanoemulsions. Ultrasound with an appropriate high frequency and ultrasonic power is transmitted to the liquid to create cavitation in the liquid. Ultrasonic cavitation has been widely used for laboratory-scale production. The synthesis of strontium titanate nanopowders utilizing a high-intensity ultrasonic probe has been described by Yashodamma *et al.* (2019). The study suggested that employing an ultrasonic-assisted sonochemical approach in laboratory research is an effective and environmentally friendly method [28]. Furthermore, Venkataravanappa *et al.* (2017) reported that the ultrasonic-assisted approach is appropriate for creating nanostructured materials and high-purity nanoparticales [29]. In another study on ultrasound-assisted emulsion production, Raviadaran *et al.* (2018) reported that ultrasound assisted the formation of a water-in-palm oil nanoemulsion. In addition, the study also compared the processing technique between an ultrasound device and a microfluidizer and found that the ultrasound used nine times less energy than a microfluidizer in creating a droplet size of 220 nm [30]. Furthermore, Tang *et al.* (2013) stated that the results of ultrasonic emulsification are competitive to those obtained using microfluidizers and other efficient high-pressure homogenizers such as orifice homogenizers [31]. Nevertheless, this method requires high-energy consumption and is difficult to execute on an industrial scale [25].

In this study, a simple rotational HCR, that is, a rotor-stator assembly reactor, was utilized to determine its effectiveness for nanoemulsion production. The rotor, which is the high-speed rotating part, was assembled with a stator, which is the stationary part of the reactor. The main purpose of using this rotor-stator-assembled cavitating device was to contribute to high-speed rotation and high shear, which are necessary characteristics for enhancing the mixing performance and cavitation

intensity of the reactor. According to Bernoulli's theory, cavitation bubbles occur when the static pressure becomes lower than the saturated vapor pressure at a constant temperature, owing to the increasing flow velocity of the liquid. Subsequently, the cavitating bubbles collapse into the liquid at high pressure, owing to the high-speed rotor. The high cavitation generation efficiency is an important factor in our operating system. According to Sun *et al.* (2021), who investigated the disinfection properties of an advanced hydrodynamic cavitation reactor on a pilot scale, a high rotating speed may lead to significant sheet and vortex cavitation zones. This is because, according to their simulation results, large separation regions and strong vortexes occurred downstream and inside the cavities, due to the high rotational speed. Therefore, a higher rotational speed can cause a higher cavitation intensity and collapse between the static and moving parts of the reactor. This is an effective achievement that facilitates the use of a rotor-stator HCR for many industrial applications such as wastewater treatment, degradation of organic compounds, food processing, and biodiesel production [32]. Oo *et al.* (2021) reported a methyl ester production process from mixed crude palm oil using a rotor-stator HCR. They compared the results of ultrasonic and rotor-stator HCRs for a two-stage process of methyl ester production. The results showed that the rotor-stator HCR saved 13.3% more energy and provided better yields than the ultrasonic reactor. Therefore, utilizing a rotor-stator HCR can efficiently reduce the energy demand [33]. Furthermore, there are many other benefits of using rotor-stator formulation reactors, such as economical effectiveness, the provision of large cavitation areas, and good scalability, which are very useful for industrial purposes [34,35].

To the best of our knowledge, no researchers have yet studied the application of a rotor-stator hydrodynamic formulation reactor for production of nanoemulsions to be used in skincare cosmetics. Therefore, the objective of this study was to produce an O/W nanoemulsion lotion using a 3D-printed rotor, which would serve as a key part of the formulation reactor, a rotor-stator-type HCR. To optimize the droplet size of the emulsion, response surface methodology (RSM) was carried out to analyze the effects of five independent variables: speed of the rotor, flow rate of mixtures, and concentrations of Span60, Tween60, and mineral oil. Furthermore, the properties of the nanoemulsions, such as droplet size, polydispersity index (PDI), pH, zeta potential, viscosity, stability, and niacin release profile from formulations, were also evaluated in this study.

2. Material and methods

2.1. Material

For production of the nanoemulsion, the oil (lipophilic) and water (aqueous) phases were utilized as feedstock to produce a coarse emulsion, as shown in Fig. 1. For use in formation of the oil phase during the emulsion process, cetyl alcohol (HLB = 15.5) and Span60 (HLB = 4.5) were purchased from P.C. Drug Center, Thailand. A moisturizer with 99.8% purity of isopropyl myristate (HLB = 10), purchased from The Real Three, Thailand, was used to coat and retain moisture in the skin. Mineral oil, DL-alpha tocopheryl acetate, and triethanolamine (99%, TEA) were obtained from Namsiang Co. Ltd. (Bangkok, Thailand). For use in formation of the aqueous phase during the emulsion process, ethylenediaminetetraacetic acid (99%, EDTA) was supplied by Sigma-Aldrich Inc., Bangkok, Thailand. Glycerin, vitamin B3 (or niacin), Tween60 (HLB = 15), carbopol Ultrez 21 polymer, and phenoxyethanol were purchased from Namsiang Co. Ltd. All chemical reagents used in the experiments were of pharmaceutical grade. Niacin release analysis was performed to evaluate the release rate of the formulated nanoemulsified niacin through the cellulose acetate membrane. All chemical

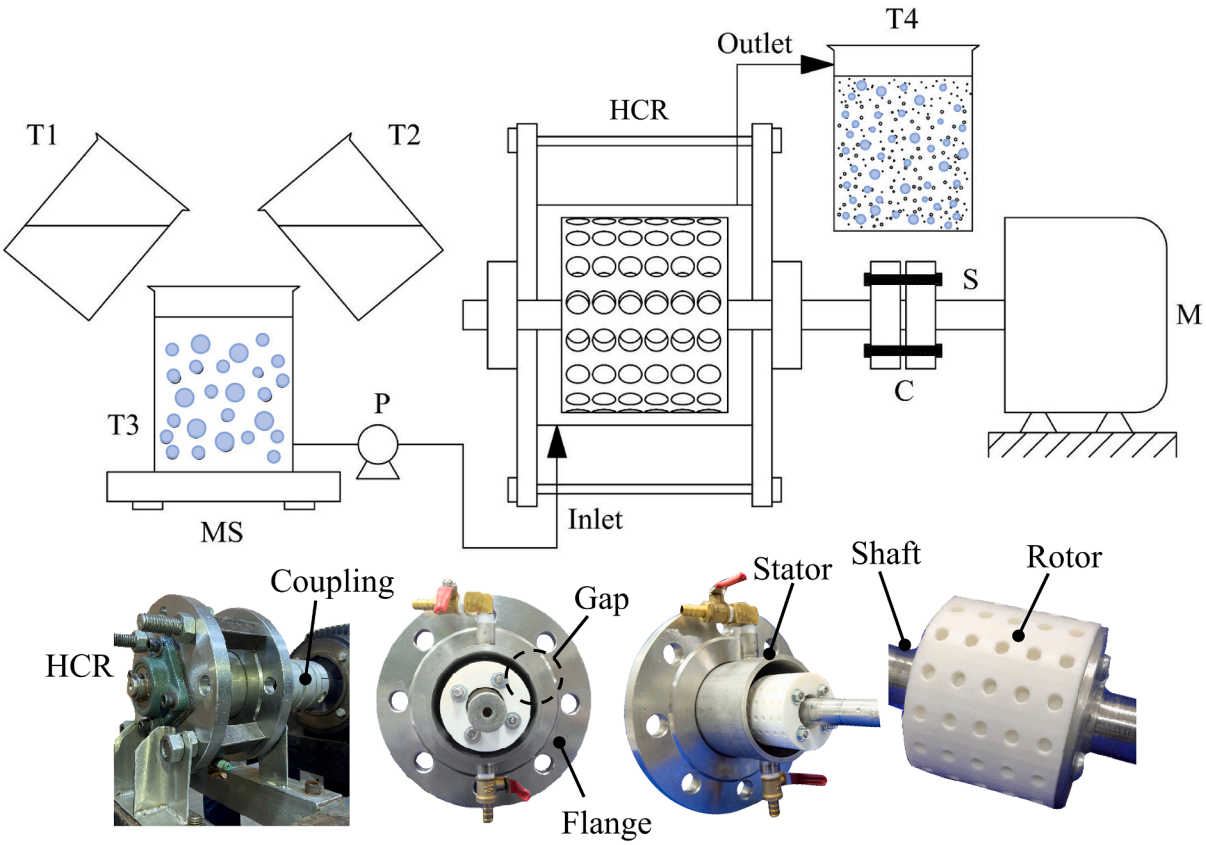

Fig. 1. A schematic diagram for the continuous production process of a nanoemulsion for a skincare lotion using a 3D-printed rotor of hydrodynamic cavitation (T1: oil phase tank, T2: aqueous phase tank, T3: coarse emulsion tank, T4: fine emulsion tank, MS: magnetic stirrer, P: chemical metering pump, HCR: hydrodynamic cavitation reactor, C: flexible shaft coupling, S: mechanical shaft, M: motor, gap: a radial gap between the rotor and stator).

reagents such as analytical-grade sodium hydroxide, potassium dihydrogen phosphate, and hydrochloric acid were obtained from Labscan Ltd. (Bangkok, Thailand).

2.2. Procedure

2.2.1. Determination of HLB

HLB indicates the water solubility of an emulsifier and categorizes emulsions as O/W or W/O [36]. The HLB numbers give an estimate of the solubility of the emulsifier that can stabilize the O/W and W/O emulsions [37]. To evaluate the optimal HLB emulsifier mixtures, the HLB numbers of the emulsions can be calculated from their weight proportions in the mixtures [38]. In this study, the HLB numbers were calculated using Eq. (1) [39,40]. Most emulsifiers have HLB values in the range of 0–20, which are determined from their molecular structures. Furthermore, the HLB numbers required for an O/W emulsifier are in the range of 8–18 [36,41]. In this experiment, the required HLB was optimized to be in the range of 11–12, which varied depending on the HLBs of the various components employed in the emulsion formulations [37,38,42]. The HLB number was modulated by varying the weight percentage of the three compounds of pharmaceutical-grade cetyl alcohol, isopropyl myristate, and mineral oil, as well as, the two surfactants of Span60 and Tween60.

$$HLB_{emulsion} = \frac{\sum HLB_i M_i}{\sum M_i} \quad (1)$$

where, HLB_i is the value that allows for enough solubility of the emulsifier to stabilize the O/W and W/O emulsions, and M_i is the percentage weight of the reagent.

2.2.2. Experimental setup

Fig. 1 shows the experimental diagram that represents the production process of a nanoemulsion for a skincare lotion using a hydrodynamic reactor. The hydrodynamic reactor comprises of two main components: a stator and a rotor, which operate together to generate hydrodynamic cavitation inside the hydrodynamic reactor. In this study, a HCR was used as a critical device, and the rotor inside the reactor was mixed to produce a nanoemulsion. The rotating part of the 3D-printed rotor was fabricated with polylactic acid using a high-performance 3D printer (model: Creator3, Flashforge, Zhejiang, China). The printing cost of this 3D-printed rotor is quite low, at approximately 2 USD, and thus, this processing technique has the potential to be both cost-effective and time-efficient [33]. In a previous study, long-lasting stainless steel rotors with many holes on their surfaces, manufactured using a computer numerical control machine, were recommended for the practical industrial process of biodiesel production. The cost of the stainless steel rotor was approximately 600 USD per rotor. Thus, the cost of a stainless-steel rotor is higher and involves a more complicated manufacturing process than those of a 3D-printed rotor. Furthermore, other plastic filaments, such as polyhydroxyalkanoates, bio-based polyethylene, and polyethylene terephthalate, have also been recommended for use in cosmetic production [43]. However, the features and conditions of printing must be studied using a 3D printer that is capable of producing cosmetics with these plastic filaments. The dimensions of the rotor used in this study were 60 mm in diameter and 46 mm in length. A rotor surface was designed with 80 spherical holes, to create cavitation. The diameter and depth of the holes were both fixed at 4 mm, as shown in Fig. 1. The stationary part of the stator had an inside diameter of 80 mm and an outer diameter of 90 mm. Therefore, the gap between the rotor and the stator was fixed at 10 mm. To get an estimate of the cavitation number (CN) in HCR, it can be considered to evaluate the cavitation intensity using Eq. (2) [44,45]. The vapor pressure of the liquid in this calculation was related to water, because water is the highest vaporizing solution in the mixture used in this study.

$$CN = (P_2 - P_v)/(0.5 \times \rho \times v^2) \quad (2)$$

where P_2 is the downstream pressure at the outlet of the reactor, P_v is the vapor pressure of the flowing liquid, ρ is the density of the flowing liquid, and v is the velocity of the liquid on the surface of the rotor. For the optimal condition, the CN was calculated as $(101325–12350)/(0.5\times982\times11.0^2) = 1.5$, using Eq. (2) when $P_2 = 101325$ Pa (in this case), $P_{v,water} = 12350$ Pa at 50 °C, $\rho_{water} = 982$ kg/m^3 at 50 °C, and $v = 11.0$ m/s at 3500 rpm. In addition, the surface velocity at $n = 3500$ rpm (under optimal condition) was calculated as $v = r\omega = 0.03\times366.5 = 11.0$ m/s, when $\omega = 2\pi n = 2\pi(3500/60) = 366.5$ rad/s, when radius of rotor (r) $= 0.06/2 = 0.03$ m.

In this study, the CN was 1.5 at the optimal condition, which was considered by utilizing the vapor pressure of water in the nanoemulsion formulation. Commonly, significant cavitation occurs when the cavitation number is equal to 1 or less than 1. However, Mahulkar *et al.* 2008 [47] reported that cavitation can occur at CN $\geq$ 1. Their research focused on steam bubble cavitation using a hydrodynamic cavitation device. They found that continuous bubble formation and collapse occurred when the CN was less than two. However, when the CN was greater than two, the created cavities cannot collapse [46]. To mix the emulsion formulations, the 3D-printed rotor in the cavitation reactor was rotated using an electrical motor (model: MG112MC, Grundfos, Taipei, Taiwan), to drive the rotor through the mechanical shaft, and the speeds of the rotor were controlled in the range of 1500 to 5500 rpm using an inverter (model: M201, Emerson, Shanghai, China). To dose the raw materials and chemical reactants into the HCR, the coarse emulsion was fed into the reactor using a chemical metering pump (model: DME 2–18, Grundfos alldos, Lyon, France) through the inlet valve. The emulsion was mixed in a HCR and continuously discharged through an outlet valve. Samples (30 mL) were collected at approximately 1.2 to 6 min intervals at the outlet port, which depended on the residence time of the coarse emulsion in the reactor. The residence time was varied because the flow rate of the coarse emulsion in this study was varied to determine the optimal droplet size of the emulsion. The residence time of the coarse emulsion in the HCR was calculated by measuring the volume of liquid inside the reactor chamber, including the rotor, using a graduated cylinder, according to the total volume flow rate of the mixture. In summary, the residence time is equal to the emulsion flow rate divided by the reactor volume. For example, the residence time under optimal conditions is 200 mL (the HCR volume) divided by 3.3 L/h (the coarse emulsion flow rate), which is equal to 3.6 min. All emulsions were analyzed using a Zetasizer Nano ZS analyzer to determine the mean droplet size of the nanoemulsions using dynamic light scattering (DLS). The droplet size of all formulations was optimized using RSM. Moreover, the optimal nanoemulsion formulation was collected and stored overnight to evaluate its properties such as stability at room temperature, freeze-thaw stability, pH, zeta potential, and viscosity.

2.2.3. Experimental procedure for preparation of skincare nanoemulsions

Before hydrodynamic cavitation, coarse emulsions of both phases were prepared by pre-mixing the oil phases in an oil-phase tank (T1), to blend 1 wt% of cetyl alcohol, 1 wt% of DL alpha-tocopheryl acetate, 0.5 wt% of TEA, 1–3 wt% of mineral oil, 6 wt% isopropyl myristate, and 1–3 wt% Span60, using a magnetic stirrer at 200 rpm, 65 °C for 5 min. All chemicals used in the preparation of the aqueous phase, which included 0.1 wt% of EDTA 99%, 5 wt% of glycerin, 1 wt% of niacin, 0.25 wt% of Carbopol Ultrez 21 polymer, 0.5 wt% of phenoxyethanol, distilled water, and higher-HLB surfactant of 1–3 wt% Tween60, were pre-mixed in an aqueous phase tank (T2). A magnetic stirrer (model: RCT BS104, IKA, Staufen, Germany) was used to blend both the oil and aqueous phases in each tank for 5 min at 200 rpm speed of stirrer while the temperature was maintained at 65 °C. The final stage in the coarse emulsion production was to gently pour the oil phase (T1) and aqueous phase (T2) into the coarse emulsion tank (T3), following which the tank

(T3) was further blended using a magnetic stirrer at 800 rpm, 65 °C for 60 min. The mean droplet size of the coarse emulsion was analyzed to determine the initial droplet size of the coarse emulsion before the nanoemulsion production process.

In the continuous nanoemulsion production process for use in skincare lotion, the temperature of the coarse emulsion was maintained at 50 °C in T3. The coarse emulsion was continually dosed into the rotor-stator of a HCR using a chemical metering pump at the inlet valve, under various flow rates of 2–10 L/h, until the reactor was fully filled with emulsion. Note that as the coarse emulsion started to be discharged from the exit valve of the HCR, the chemical metering pump was instantly switched off, while a high-speed motor was turned on to demonstrate this process. At the beginning of mixing in the reactor, batch mode was used, which required twice the calculated residence time of the coarse emulsion flowing through the reactor to obtain more equilibrated conditions and a fine emulsion. For example, since the residence time at optimal condition in the actual operation of the coarse emulsion inside the reactor was 3.6 min, the calculated residence time was set up to twice that value (*i.e.*, 7.2 min), to obtain more equilibrium conditions and a fine emulsion. Therefore, the outlet samples from the reactor were collected at a time interval of 7.2 min for the optimum condition. The metering pump was turned off to stop the dosing emulsion, while the rotor in the stator continued to spin. This processing step was performed in batch mode for 1.2 to 6 min, depending on the flow rate of the coarse emulsion. Subsequently, the metering pump was restarted to feed coarse emulsion into the reactor. Consequently, the nanoemulsion was continuously discharged through the output valve.

2.3. Characterization of the nanoemulsion

2.3.1. Droplet size and PDI measurements

Droplet size is known to decrease in the dispersed phase, resulting from increased physical stability in emulsions [47]. The droplet size must be less than 500 nm in diameter [48]. As the first step in examining the droplet size of the emulsion, the droplet sizes of various formulations, in the range of 1000 to 10000 nm, were observed using an optical microscope (model: CX23, Olympus, Qingdao, China). A Zetasizer Nano instrument (model: ZEN3600, Malvern Panalytical, Worcestershire, UK) was used to determine the mean droplet size of the nanoemulsions at 25 °C using the DLS technique. To prepare the sample for droplet size analysis, one gram of the nanoemulsion was diluted with 50 g of deionized water (1:50 mass ratio of nanoemulsion to deionized water). The nanoemulsion and deionized water were weighed in 120 mL sample vials on a digital analytical balance (model: AL204, Mettler-Toledo, Küsnacht, Switzerland), with an accuracy of 0.0001 g. For the analytical procedure, the diluted sample was placed into 1.5 mL plastic cuvettes in a thermostated chamber. The scattering intensity measurements were performed using a 633 nm red laser and a scattering angle of 173°, with particle sizes ranging from 0.6−6000 nm. The PDI is a tool used to accurately describe the particle size in an emulsion. PDI may range from 0 to 1, and is determined by dividing the square of the standard deviation by the mean particle diameter [49]. PDI in the range of 0 to 0.3 is considered to be acceptable for a nanoemulsion formulation [50,51].

2.3.2. pH

The pH of the skin is usually acidic, ranging from 4 to 6, while the pH of the body's internal environment is neutral to slightly alkaline, ranging from 7.0 to roughly 7.4 [52,53]. The pH of an emulsion is an extremely important characteristic that affects its absorption into the skin [10]. Furthermore, skincare products with either too high or too low pH values cause skin irritation. In several studies, researchers have found that the pH values of cosmetic products are typically in the range between 5.5 and 8.0, depending on the ingredients in the emulsion formulation [11]. Alkaline lotions are applied to enhance the dispersion through the skin, heal stressed skin, and firm slacked connective tissue, because they allow for higher acidity counteraction and better effectiveness of the skin's enzyme activity [54,55]. A slightly basic pH of 7.4 is excellent for daily grooming, as it does not dry out the skin. The pH of the emulsion formulations developed in this study was determined using a digital pH meter (model: SevenCompact™ pH/Ion meter S220, Mettler-Toledo AG, Zürich, Switzerland). For sample preparation, 1 g of the nanoemulsion was diluted with 9 g of deionized water to achieve the desired concentration. The pH was determined by simply dipping a glass electrode probe into the sample.

2.3.3. Zeta potential

The zeta potential value is considered to be a useful index for describing the condition of the nanoparticle surface and determining its long-term stability [56]. Nanoemulsion formulations with electrical potentials greater than or less than −30 mV are considered stable colloidal suspension systems with excellent stability against nanoparticle aggregation [57,58]. To enhance the zeta potential value, surfactants must be added to the O/W and W/O emulsions [59,60]. For analyzing the zeta potential of the emulsions, a Zetasizer Nano ZS analyzer was used to measure the conductivity of the nanoemulsions at 25 °C using the laser Doppler electrophoresis technique. An electric field between +200 and −200 mV was applied to the emulsion. To prepare the samples, a 1:50 mass ratio of nanoemulsion to deionized water was prepared to analyze the conductivity. The sample was loaded into a 1.5 mL folded capillary zeta potential cell in a thermostated chamber, and conductivity was measured using a gold-plated electrode (model: DTS1060, Malvern Instruments, Massachusetts, USA).

2.3.4. Viscosity measurement

Viscosity is an essential factor when considering the type of lotion. Although increasing the viscosity of the gels improves the stability of the emulsion, it also decreases the ability of the product to be absorbed and pass through the skin [61]. The viscosity of the final product is affected by various ingredients in the emulsion formulation, as well as, the mixing process. The properties of all the ingredients used in emulsion formulations are reported in Table 1. The viscosities of the different formulations were determined in the units of centipoise (cP) using a viscometer (model: LVT, Synchro-Lectric Viscometer, Brookfield, Massachusetts, USA) with the T-bar spindle maintained at a speed of 6 rpm at 25 °C.

2.3.5. Assessment of emulsion stability

In the next part of the study, the stability of the emulsion against phase separation under various weather conditions and upon shelf storage was tested. The physical appearance of the samples were examined to detect eye-visible structures and phase separation after 1, 30, 60, and 90 d of storage. Six heating-cooling cycles were performed between the temperatures of −4 °C and 45 °C, with a storage time of 24 h, for freeze-thaw cycle stress testing [60]. After each cycle, the stability of the nanoemultions was determined by evaluating their physical appearance. The appearance, pH, viscosity, and droplet size were also determined after 90 d of storage to confirm the long-term shelf-life. The physical appearance of the nanoemulsions was evaluated after each cycle to assess their stability. After 90 d of storage, the appearance, pH, viscosity, and droplet size were analyzed to validate their characteristics.

2.3.6. Evaluation of niacin released from formulations

The experiment was conducted using a Franz diffusion cell (model: 57-6M, Hanson, California, USA). The diffusion area of the receptor chamber was 1.77 cm^2, with a total capacity of 11.4 mL [66]. A cellulose acetate membrane with a molecular weight cut-off (MWCO) of 3500 Da was prepared for the space between the donor and receptor compartments, while carefully avoiding the formation of bubbles in the gap. The receptor compartment was filled with phosphate buffer (pH 7.4) to maintain sink conditions [60]. Subsequently, 1 g of the niacin emulsion

Table 1
Properties of raw materials and chemical reagents.

Property	Oil phase					
	Cetyl alcohol [62]	IPM [62]	Mineral oil [62]	Vitamin E [62]	Span60 [62]	TEA [63]
Appearance	crystals	liquid	liquid	viscous liquid	colored flakes	liquid
Color	white	clear	colorless	yellow	cream	clear
Melting point (°C)	49	−5	−9 max	−28	54–57	
Boiling point (°C)	344	193	315 min	224	464.84	336.1
Flash point (°C)		110 min	185 min	110 min	110 min	179 min
Solubility in water (g/L)	insoluble	immiscible	insoluble	immiscible	insoluble	immiscible
Refractive index	1.428	1.434	1.467	1.497	1.459	1000 min
Density (g/mL)		0.85	0.85	0.96	1	
Viscosity (cP)	53 at 75 °C	1.25–1.75	15.3 at 40 °C			934 at 20 °C
pH		5.1		6–8	5.5	
HLB	15.5	11.5	10		4.7	
	Water phase					
	EDTA [62]	Vitamin B3	Carbopol Ultrez 21 [65]	Glycerin [62]	Tween60 [62]	Phenoxy ethanol [62]
Appearance	crystalline	white [62]	powder	viscous liquid	oily liquid	liquid
Color	white	translucent crystals [64]	white	clear	yellow	clear
Melting point (°C)	250	236 [62]		20	45–50	11–13
Boiling point (°C)	434.18			290	802.68	247
Flash point (°C)	400 min	193 [62]		160	190	127
Solubility in water (g/L)	0.5			500 min at 20 °C	100	30
Refractive index	1.363			1.474	1.474	1.539
Density (g/mL)	0.86	1.473 [62]		1.25	1.044	1.107
Viscosity (cP)				1.412		20.5 at 25 °C
pH	2.5	2.7 [62]	3	5.5–8	5.5–7.7	7
HLB					15	

or nanoemulsion was applied after 30 min of equilibration in a water bath. The receptor compartment was adjusted to 37 °C and the solution was stirred constantly at 500 rpm for the whole period of experimental processing. At time intervals of 1, 2, 3, 6, 9, and 12 h, 1 mL of the receiving medium was withdrawn and replaced with an equal amount of new receptor medium. The niacin content was analyzed using a UV-visible spectrophotometer (model: UV-1800, Shimadzu, Kyoto, Japan), and the niacin release profile was estimated. Eq. (3) shows the cumulative amount (Q_t) of niacin released per unit area [67].

$$Q_t = \frac{C_t V + \sum_{i=0}^{n-1} C_i S}{A} \tag{3}$$

where C_i is the concentration of niacin present in the receiving medium at the i^{th} sampling time (μg/mL), C_t is the niacin concentration of the receiver solution at each sampling time, A is the effective release area of the diffusion cell, V is the sample volume taken from the receptor compartment, and S is the volume of the sample withdrawn.

2.3.7. Determination of niacin content using a UV-spectrophotometer

The niacin content in phosphate buffer (pH 7.4) was measured using a UV-visible spectrophotometer, to determine the release of niacin from the formulations. Niacin content was evaluated according to the method described by Chanda *et al.* (2017), with slight modifications. Six solutions (1–40 g/mL) of different concentrations were produced from a standard stock solution of niacin for the linearity study. The permeability of these solutions was measured at the wavelength of 262 nm against phosphate buffer pH 7.4 as a blank, and the collected data were used to create a calibration curve for the permeability measurements [68].

2.4. Experimental design

The different independent parameters were varied to formulate the nanoemulsion for the skincare product using a HCR with a 3D-printed rotor. The coarse emulsion from T3 was fed into the HCR, and five independent variables, including speed of the rotor (R, 1500–5500 rpm), flow rate (Q, 2–10 L/h), Span60 concentration (S, 1–3 wt%), Tween60 concentration (T, 1–3 wt%), and mineral oil concentration (M, 1–3 wt %), were varied to determine the optimized conditions for reducing the droplet size of the nanoemulsion formulation using a HCR. Table 2 shows the ranges of the independent variables used in the nanoemulsion formulation employing HCR. Rotatable central composite inscribes were used for the five independent variables; the axis parameter (a_x) was equal to 2. Thus, their coded independent levels for the emulsion droplet size were −2, −1, 0, +1, and +2. The experiment included a total of 30 runs, with 26 experimental points and 4 central points, as shown in Table 3. The response variable was the droplet size of the emulsion formulation. A second-order polynomial regression equation was applied to fit the experimental data [69]. In the regression analysis, analysis of variance (ANOVA) was performed to evaluate the influence of independent factors on the dependent variable. The probability values (p-values) of the models, lack of fit, and coefficient of determination (R^2) were examined to evaluate the suitability of the predictive model. The experimental design and statistical data analysis were performed using Essential Regression and Essential Experimental Design.

3. Results and discussion

3.1. RSM and statistical analyses

The mean droplet sizes of the nanoemulsions obtained from the 30 experimental runs are shown in Table 3. The droplet size ranged from 383.3 to 1485.0 nm. A second-order polynomial model was predicted for a continuous nanoemulsion formulation using rotor-stator hydrodynamic cavitation. Multiple regression analysis was used to create the

Table 2
Coding of independent variables for the continuous nanoemulsion production process.

Independent variable		Varying levels				
		−2	−1	0	+1	+2
R	Speed of rotor	1500	2500	3500	4500	5500
Q	Flow rate (L/h)	2	4	6	8	10
S	Span60 (wt%)	1	1.5	2	2.5	3
T	Tween60 (wt%)	1	1.5	2	2.5	3
M	Mineral oil (wt%)	1	1.5	2	2.5	3

Table 3
DOE and results of continuous nanoemulsion production process.

Run	R (rpm)	Q (L/h)	S (wt%)	T (wt%)	M (wt%)	D (nm)
1	3500	6	2.0	2.0	2.0	627.2
2	3500	6	2.0	2.0	2.0	637.3
3	3500	6	2.0	2.0	2.0	647.4
4	3500	6	2.0	2.0	2.0	617.8
5	1500	6	2.0	2.0	2.0	701.0
6	5500	6	2.0	2.0	2.0	383.3
7	3500	2	2.0	2.0	2.0	528.0
8	3500	10	2.0	2.0	2.0	618.9
9	4500	4	1.5	1.5	1.5	890.1
10	4500	4	2.5	2.5	1.5	407.3
11	4500	4	1.5	2.5	2.5	465.8
12	4500	4	2.5	1.5	2.5	640.9
13	2500	4	1.5	2.5	1.5	662.0
14	2500	4	2.5	1.5	1.5	733.7
15	2500	4	1.5	1.5	2.5	655.8
16	2500	4	2.5	2.5	2.5	481.1
17	3500	6	2.0	2.0	1.0	783.1
18	3500	6	1.0	2.0	2.0	928.9
19	3500	6	2.0	1.0	2.0	841.1
20	3500	6	2.0	3.0	2.0	550.4
21	3500	6	3.0	2.0	2.0	705.9
22	3500	6	2.0	2.0	3.0	657.1
23	4500	8	1.5	2.5	1.5	518.8
24	4500	8	2.5	1.5	1.5	601.0
25	4500	8	1.5	1.5	2.5	573.7
26	4500	8	2.5	2.5	2.5	489.3
27	2500	8	1.5	1.5	1.5	1119.0
28	2500	8	2.5	2.5	1.5	520.9
29	2500	8	1.5	2.5	2.5	916.8
30	2500	8	2.5	1.5	2.5	725.4

Note: R, speed of the rotor; Q, flow rate; S, Span60; T, Tween60; M, mineral oil; D, droplet size.

prediction model in Eq. (4), which was derived from experimental data and model fitting. Table 3 and Table 4 show the coefficients of the fitted models, *p*-values for each term, and ANOVA, respectively.

Table 4
Coefficients in the fitted response surface model and ANOVA.

Coefficients			Value	*p*-value	
β_0			3638.944	0.0000001355189	
β_1			144.498	0.0019982120958	
β_2			0.169	0.0159516157175	
β_3			−1264.058	0.0000010316524	
β_4			−1195.513	0.0000014636728	
β_5			−791.708	0.0000003551361	
β_6			−5.554	0.0038429641791	
β_7			−0.030	0.0000058273040	
β_8			24.687	0.0106694074595	
β_9			–23.813	0.0130674724526	
β_{10}			20.688	0.0267913885482	
β_{11}			0.000	0.0003823994915	
β_{12}			0.073	0.0007266858357	
β_{13}			57.783	0.0399704042265	
β_{14}			162.900	0.0002831999692	
β_{15}			248.000	0.0000046278742	
β_{16}			155.083	0.0000363321659	
ANOVA					
Source	SS	MS	F_0	F_{crit}	DOF
Regression	772608	48288.0	43.93	2.51 ($F_{0.05,16,13}$)	16
Residual (Error)	14288.9	1099.1			13
Lack-of-Fit Error	13799.7	1380.0			10
Pure Error	489.21	163.07			3
Total	786897				29

Note: Coefficient of determination (R^2) = 0.982; Adjusted coefficient of determination ($R^2_{adjusted}$) = 0.959. DOF, degrees of freedom; SS, sum of squares; MS, mean square.

$$D = \beta_0 + \beta_1 Q + \beta_2 R + \beta_3 M + \beta_4 S + \beta_5 T + \beta_6 Q^2 + \beta_7 QR + \beta_8 QM + \beta_9 QS + \beta_{10} QT + \beta_{11} R^2 + \beta_{12} RS + \beta_{13} M^2 + \beta_{14} MS + \beta_{15} MT + \beta_{16} S^2 \quad (4)$$

where, the variables are used to represent the independent variables in the nanoemulsion formulation process; R, speed of the rotor (rpm); Q, flow rate (L/h); S, Span60 concentration (wt%); T, Tween60 concentration (wt%); M, mineral oil concentration (wt%); β, fixed coefficient.

The R^2, adjusted coefficient of determination ($R^2_{adjusted}$), and ANOVA revealed significant results for the predictive model at the 95% confidence interval, as shown in Table 3. The *p*-values were used to prove the statistical significance of each term in the prediction model, and the *F*-test was used to test the overall significance of the predictive model. When *p*-values were considered, the statistical significance of each term in the model was evaluated in terms of their *p*-values. A statistically significant result is described as one in which the *p*-values are less than 0.05 when the 95% confidence level is used. The experimental design list and results are described in Table 3. The R^2 and $R^2_{adjusted}$ values of droplet size in the nanoemulsion were 0.982 and 0.959, respectively. The predicted model is considered highly correlated when the statistical values are higher than 0.80 [70]. Therefore, the RSM model of the continuous nanoemulsion process was used to represent the relationships between the independent and dependent variables. Each independent factor was significant in terms of its *p*-values, but the linear term, T, had the lowest *p*-value. Therefore, Tween60 is the most essential for continuous nanoemulsion production using hydrodynamic cavitation. Mineral oil and Span60 ranked second and third, for the terms of β_3M and β_4S, respectively, and these two terms had almost similar levels of significance. Because Tween60 is an emulsifier, it was used to improve the microstructure of the emulsion. The droplet size was reduced by increasing the number of droplets in the dispersion phase [71]. Similar results were obtained by Basiri *et al.* (2017), who studied the improvement and validation of niosomes containing α-tocopherol. Different molar ratios of Span60 to Tween60 were varied to study the efficiency of encapsulation in the food industry. They found that the particle sizes of niosomes in the nanoemulsions were 106.8, 176, and 157 nm, when Span60 to Tween60 ratios of 1:1, 2:1, and 3:1, respectively, were used. Therefore, the droplet size in the nanoemulsion decreased when a higher Tween60 amount was blended into the emulsion formulations [72]. Junyaprasert *et al.* (2021) created niosomes by means of encapsulation of ellagic acid. Upon varying the ratio of Span60 to Tween60, the smallest droplet size was observed when a high concentration of Tween60 was blended into the niosomes. In contrast, the formulation containing Span60 had the largest droplet size as compared to those in formulations with different surfactant ratios [73]. The relationships between the independent and dependent variables of β_{15}MT and β_7QR were ranked fourth and fifth, respectively, in quadratic terms. ANOVA was also performed on the prediction model, to evaluate the significance of each model, as shown in Table 3. To evaluate model adequacy, the *F*-test statistic (F_0) value should be higher than the critical value (F_{crit}). Therefore, the prediction model for the droplet size of the nanoemulsion was found to be statistically significant.

3.2. Response surface plots

The contour plots obtained from the predictive model in Eq. (4) were used to describe the interactions between the dependent variable (droplet size) and independent variables (rotor speed, flow rate, and concentrations of Span60, Tween60, and mineral oil) for a continuous nanoemulsion formulation process using a HCR, as shown in Fig. 2.

3.3. Optimum conditions for continuous nanoemulsion formulation

Optimization of the process of continuous nanoemulsion formulation using a HCR was carried out using the essential regression and solver add-in in Microsoft Excel, based on the experimental results. To determine the optimal conditions, the five independent variables of rotor

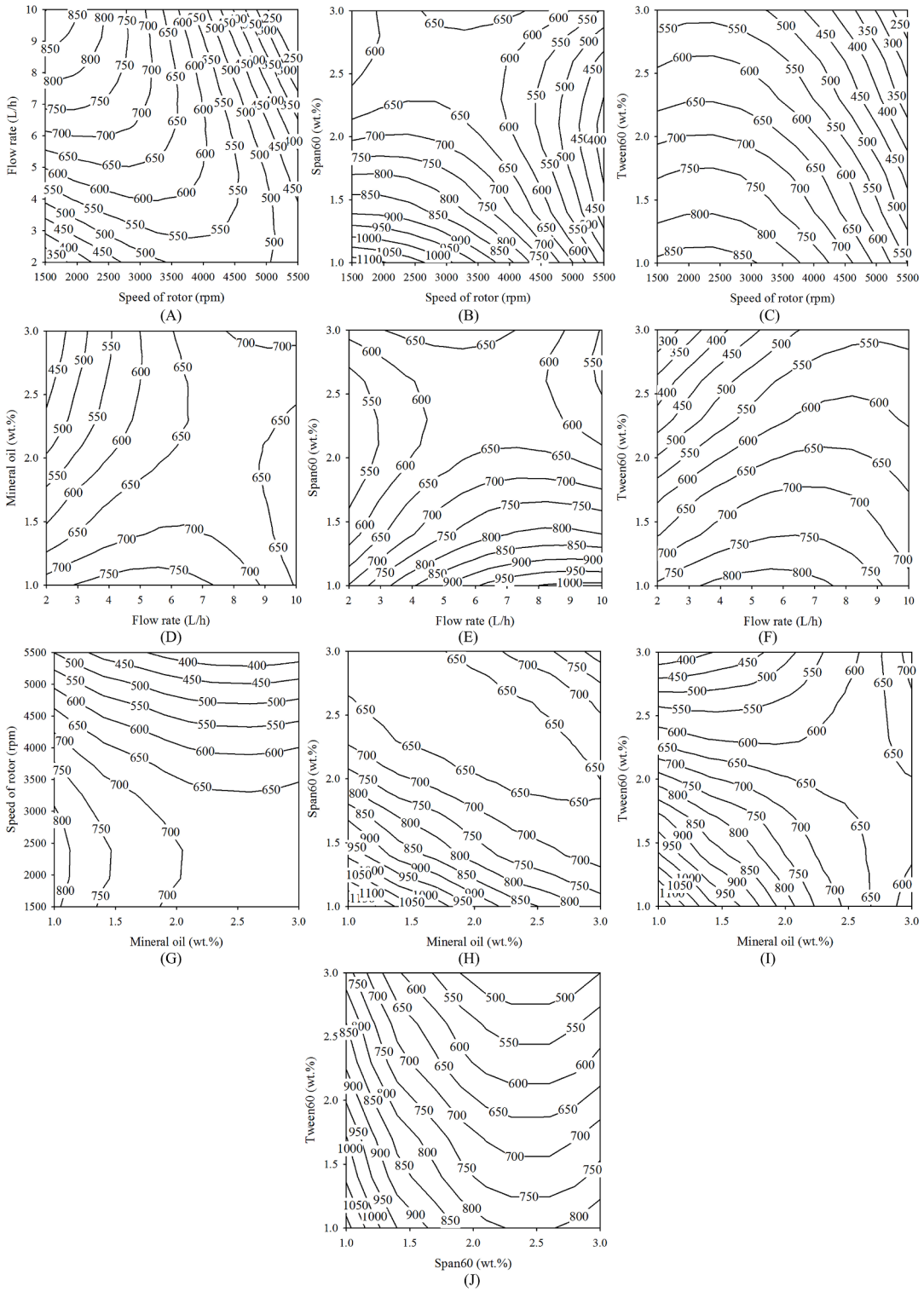

Fig. 2. Contour plots of the optimized conditions for continuous process interactions of (A, B, and C) speed of rotor with flow rate and concentrations of Span60 and Tween60; (D, E, and F) flow rate with concentrations of mineral oil, Span60, and Tween60; (G, H, and I) concentrations of mineral oil with speed of rotor, Span60, and Tween60; (J) concentration of Span60 with concentration of Tween60, on the reduction of droplet size of emulsions.

speed, flow rate, and concentrations of Span60, Tween60, and mineral oil were set in the ranges shown in Table 2, while the droplet size of the emulsion was set as the dependent variable. The results showed that a droplet size of 300 nm was achieved under the recommended conditions of rotor speed of 3500 rpm, flow rate of 3.3 L/h, 2.36 wt% Span60, 3.00 wt% Tween60, and 1.76 wt% mineral oil. Subsequently, the recommended condition from the predictive model of the nanoemulsion formulation was verified using an experiment to confirm the droplet size of the emulsion using a Zetasizer Nano ZS analyzer. The results showed that mean droplet sizes of 366.4 nm and 491.7 nm were achieved at 1 h and 90 d, respectively. The droplet size in the nanoemulsion was approximately 300 nm, as predicted by the model. Finally, PDI is an important parameter to determine the homogeneity and stability of the formulated nanoemulsion. The PDI values of the nanoemulsions under

the recommended conditions were 0.298, 0.302, 0.365, 0.398, and 0.452 at 1 h, 1 d, 30 d, 60 d, and 90 d, respectively. PDI values increased linearly with increasing storage duration. With respect to the relationship between droplet size and PDI, the droplet size of the nanoemulsion increases as the storage time increases and corresponds to an increase in PDI [50].

3.4. pH study

The pH of cosmetics affects their absorption on the skin, and the degree of acidity (pH) is an extremely significant characteristic of cosmetic products. Cosmetics with very high or low pH are prone to irritation. The pH values of the emulsion samples were measured using a digital pH meter. The results showed that the pH values from 30 experimental runs ranged between 7.44 and 7.61 for the freshly prepared alkaline emulsion. These pH ranges are within the recommended pH range for cosmetic preparations, which is from 5.5 to 8.0 [11]. TEA was used to properly adjust the pH values of the lotion such that they were close to neutral. Increasing the alkalinity of the emulsion allowed for adjustment of the pH value of the emulsion [10]. In general, a slightly basic pH of 7.4 does not dry out the skin and is suitable for frequent grooming. Therefore, topical treatments should have a pH value in this range [55,74]. The final pH of the skincare lotion was 7.4 under the recommended conditions. Several studies have reported that nanoemulsions with a pH of 7.4 do not cause skin irritation [8,9].

3.5. Zeta potential study

Zeta potential of the emulsions was examined using a zeta potential analyzer at 25 °C, to determine the phase system of the nanoemulsion [75]. All formulations produced a zeta potential greater than −30.8 mV, and the zeta potential of the fresh lotion from 30 experimental runs ranged between −83.1 and −30.8 mV for the O/W emulsion, depending on the formulation. To avoid the re-coalescence of nanoemulsion aggregates, zeta potentials greater than +30 mV and less than −30 mV are recommended in an emulsion [57,58]. The zeta potential of the nanoemulsion was found to be −62.8 mV under the recommended conditions, as shown in Table 5.

3.6. Viscosity study

A viscometer with a T-bar spindle maintained at a speed of 6 rpm and temperature of 25 °C was used to determine the viscosity of the lotion formulations. Viscosities in the range of 4680 to 52416 cP were found upon maintenance for 1 h at 25 °C for 30 runs. Under the recommended conditions, the viscosities of the nanoemulsion were 12948 cP (at 1 h) and 13182 cP (at 90 d), which satisfy the recommendations of the Food and Drug Administration (according to which, the viscosity of a good lotion should be less than 30000 cP) [10]. Similar reports have been described by Anggelina *et al.* (2021) and Weiss (2011), who reported that the viscosity of a lotion should be less than 30000 cP [9,76].

Table 5
Properties of the nanoemulsion under the recommended conditions.

Property	Result
Appearance	clear liquid single phase
Color	milky
Conductivity (mV)	−62.8
Viscosity (cP) at 25 °C	12948
pH	7.4
HLB	11.1
PDI	0.298
Long term stability at 30 °C (~90 d)	liquid one phase
Freeze–thaw cycle stress tests (six cycles)	liquid one phase
Mean droplet size (nm) at 1 h	
Hydrodynamic cavitation	366.4
Ultrasonic cavitation	373.5
Magnetic stirrer	1879
Cumulative amount of niacin release at 12 h (μg/cm^2)	
Hydrodynamic cavitation	4335.8
Ultrasonic cavitation	4156.3
Magnetic stirrer	3545.4

3.7. Stability and droplet size

Physical stability tests were carried out by assessing the structures visible to the eye and phase separation at a storage temperature of 30 °C. After monitoring the phase stability of the emulsions for 1 h, the long-term stability of all emulsion formulations was investigated after storage for 30, 60, and 90 d. The phase behavior analyses of emulsions from 30 experimental runs at 30 °C are shown in Fig. 3. Physical appearance can be categorized into three types of phase behavior, as shown in Fig. 3. In Fig. 3A, the phase behavior shown is that of a homogenous single liquid phase. The viscosities of the emulsions ranged from 4680 to 23712 cP at 25 °C. Furthermore, this phase separation type is a homogenous phase with no phase separation; the emulsion becomes milky white after 90 d of storage at 30 °C. Fig. 3B shows the unstable emulsion formulations that separated into water and oil phases after storage for durations between 30 and 90 d, which may be caused in nearly all formulations having droplet sizes larger than 550 nm. Because the droplet size of a nanoemulsion will impact the long-term stability of the emulsion, the smaller droplet size in a nanoemulsion is better than that in an emulsion obtained by means of conventional emulsion formulation [77]. These results are similar to those obtained by Ribeiro *et al.* (2015), who studied the characteristics of cosmetic nanoemulsions consisting of *Opuntia ficus-indica* (L.) mill extract, which is used as a moisturizing agent. The study mentioned that droplet size is one of the most significant variables required to determine applicability and stability. The droplet size of the nanoemulsion increased slightly with increasing storage time [78]. Fig. 3C shows the last phase type, a liquid phase with air bubbles, which is a highly viscous lotion. Freeze-thaw cycle testing was conducted for six cycles, with a storage duration of 24 h at each temperature, to verify the stability of the nanoemulsion product during the heating-cooling cycles of the recommended formulation between −4 °C and 45 °C. This is adequate for delivery to the customer and allows for stability of the product during transit under different conditions. There was no change in the phase separation of the nanoemulsions during the severe high- and low-temperature changes. The stability study demonstrated that nanoemulsions for skincare products were able to maintain their integrity without phase separation in the liquid phase, as shown in Fig. 3A. As a result, employing hydrodynamic cavitation and appropriate reagents was in good agreement for formulation of nanoemulsions under the recommended conditions. Stability studies have shown that nanoemulsions can maintain their integrity in the liquid phase without phase separation. For preliminary observations of droplet size after 1 h of blending the formulations using various blending methods such as a magnetic stirrer, ultrasonic cavitation, and rotor-stator hydrodynamic cavitation, under the recommended conditions for formulation of the lotion, the droplet sizes in the range of 1000 to 10000 nm were found to be oil droplets in the emulsions, as shown in Fig. 4. To check if the droplet size of the recommended formulation ranged in the nano size, the Zetasizer Nano instrument was used to determine the mean droplet size of nanoemulsions using different blending techniques. The emulsion prepared using a magnetic stirrer (Fig. 4A) displayed a droplet size of 1879 nm. The nanoemulsion formulation prepared using ultrasonic cavitation (Fig. 4B) had a droplet size of 373.5 nm, while the last one prepared using hydrosonic cavitation (Fig. 4C) presented a droplet size of 366.4 nm, as reported in Table 5. The smallest droplet size distribution was obtained in the blending method with rotor-stator hydrodynamic cavitation, because the HCR machine contributed to high-speed rotation and high shear, which are necessary characteristics for enhancing the mixing performance and cavitation intensity while running the process inside the

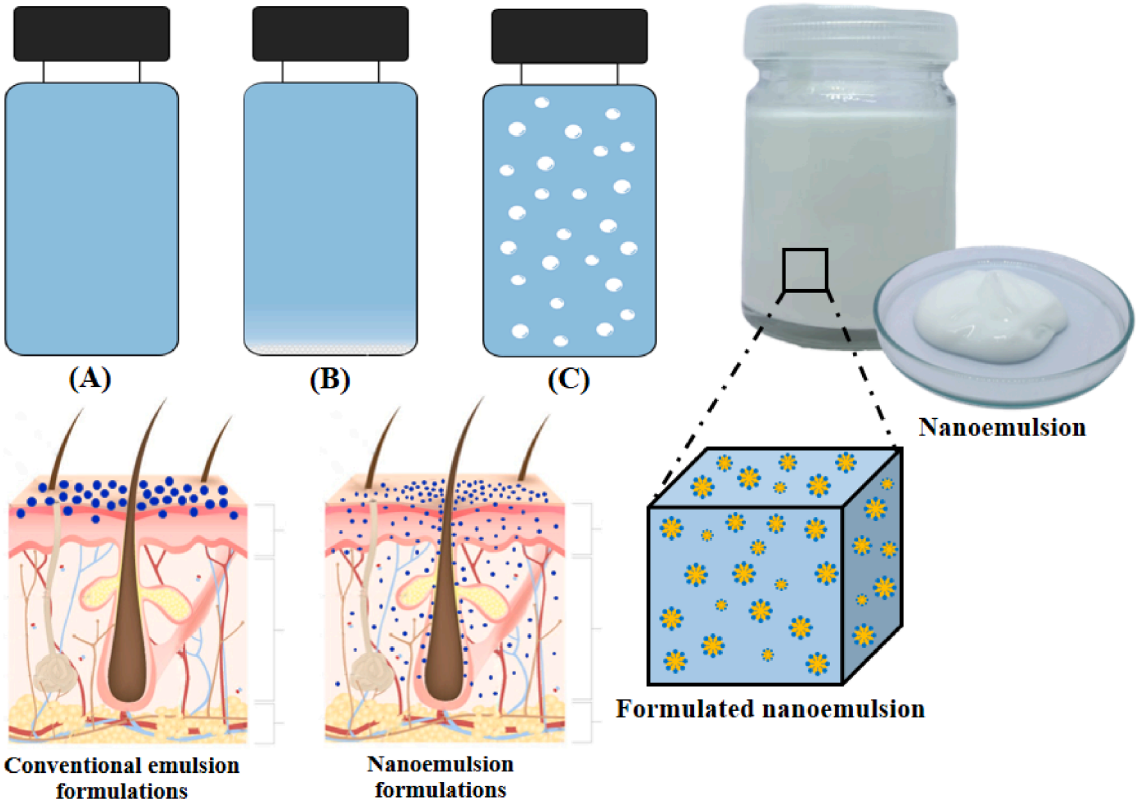

Fig. 3. Phase separation types observed in the emulsion, (A) liquid single phase, (B) unstable emulsion, and (C) liquid single phase with air bubbles.

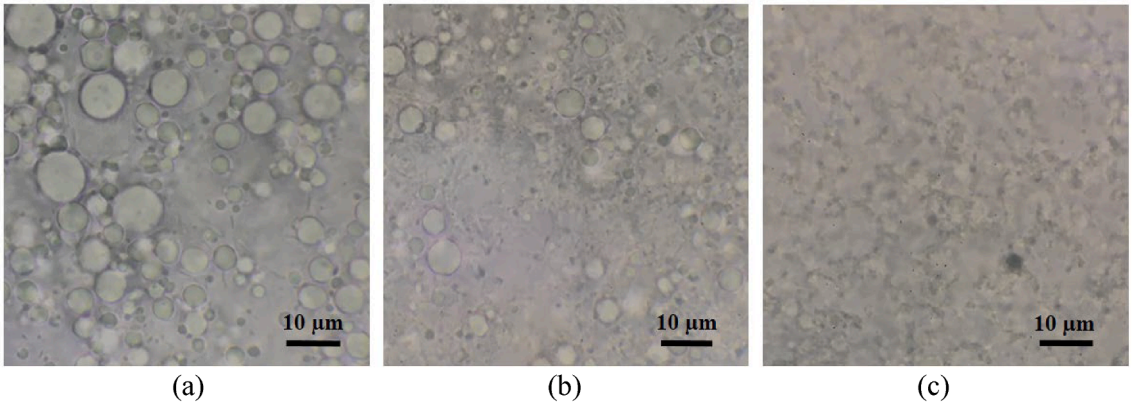

Fig. 4. Optical microscopy images of emulsions prepared using (A) magnetic stirrer, (B) ultrasonic cavitation, and (C) rotor-stator hydrodynamic cavitation.

reactor. Similar reports were described by Ashokkumar *et al.* (2011) [34], and Oo *et al.* (2021), who mentioned that hydrodynamic cavitation is an alternative to acoustic cavitation, as it is suitable for industrial mass production [33]. Furthermore, the rotor-stator type of reactor is particularly well suited for industrial applications owing to the extensive utilization of the cavitation zone, low cost of equipment, and ease of scaling [35].

3.8. Release profile of niacin emulsion and nanoemulsion formulations

The release profiles of three formulations, one niacin emulsion and two niacin nanoemulsions, were investigated under three formulation conditions. The niacin content was determined using a UV-visible spectrophotometer at λ_{max} of 262 nm. Niacin was found to be linear within a concentration range of 1–40 µg/mL and exhibited a correlation coefficient of 0.9999. The release profiles of all formulations are shown in Fig. 5. The niacin emulsion was prepared using a magnetic stirrer, and had a droplet size of 1879 nm. One of nanoemulsion formulation was prepared using a hydrodynamic instrument, which resulted in a droplet size of 373.5 nm, while the other was prepared using a hydrodynamic instrument, which resulted in a droplet size of 366.4 nm. Both nanoemulsion formulations had similar droplet sizes, but the emulsion was approximately three times larger in size than the nanoemulsion. The molecular weight of niacin is 123.11 g/mole, which means that it is a small molecule that can pass easily through the cellulose acetate membrane, which has a MWCO of 3500 Da. The niacin emulsion had a larger droplet size than both the nanoemulsions, and after 2 h of release, all the formulations showed similar and very high release, because of the smaller droplet size compared to the pore size of the membrane. The effects of emulsion droplet size on the different emulsification methods were investigated by measuring the cumulative amount of niacin released at various time-points, of 1, 2, 3, 6, 9, and 12 h, as shown in

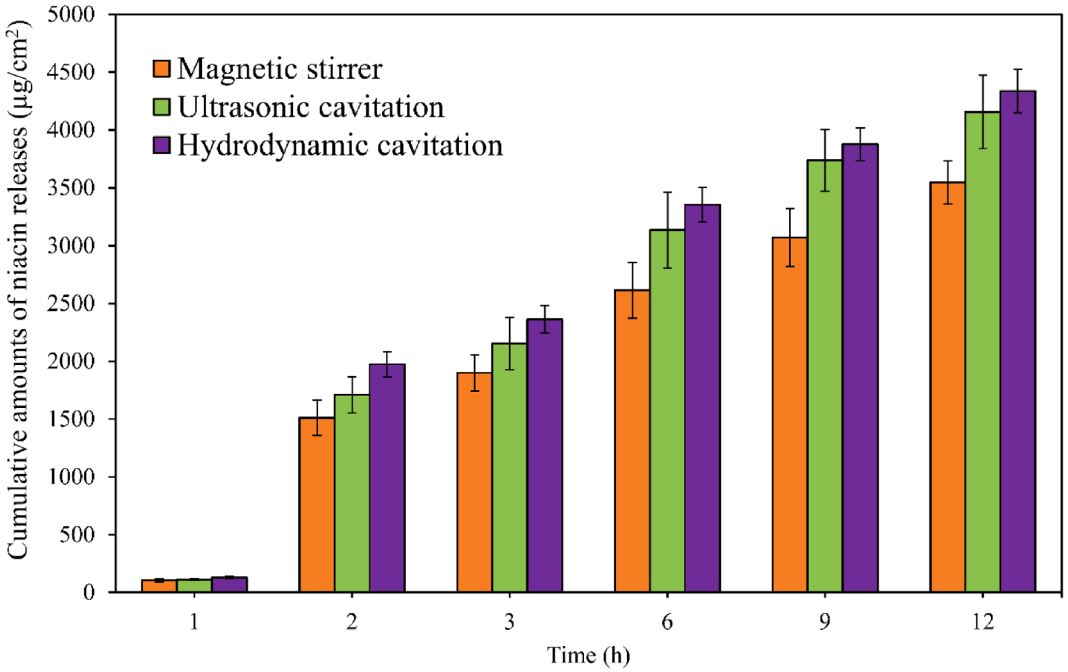

Fig. 5. Release profile of niacin emulsion and nanoemulsion formulations at various time-points, upon using different mixing methods.

Fig. 5. The cumulative amounts of niacin released increased sharply to 3545.4, 4156.3, and 4335.8 μg/cm^2 from 1 to 12 h, upon use of magnetic stirrer, ultrasonic cavitation, and hydrodynamic cavitation, respectively, as shown in Table 5. Therefore, after longer durations of release, the nanoemulsion formulations showed higher release than the emulsion. It was observed that the nanoemulsion prepared using the HCR gave the highest cumulative release from the formulation after 12 h. The lower release of the emulsion after longer durations may be due to the accumulation of larger sized particles on the pores of the membranes, which leads to obstruction of the pores, further reducing the flow of formulations.

4. Conclusions

In this study, a rotor-stator HCR containing a 3D-printed rotor was successfully applied to the production process of a nanoemulsion to be used in a skincare lotion. The results showed that a droplet size of 366.4 nm was achieved at a rotor speed of 3500 rpm, flow rate of 3.3 L/h, Span60 concentration of 2.36 wt%, Tween60 concentration of 3.00 wt %, and mineral oil concentration of 1.76 wt%. The PDI, which is an important parameter to determine the homogeneity and stability of the formulated nanoemulsion, was 0.298 at the optimum conditions, which was within the acceptable range for nanoemulsion formulations. Moreover, the pH values for the nanoemulsions generated under all the experimental conditions were in the range of 7.44–7.61, which are also acceptable values for cosmetic product formulations. Another important parameter, zeta potential, was found to be −62.8 mV under the recommended conditions, which met the conditions for nanoemulsion formulations with excellent stability. The viscosity of the final product was 12948 cP after 1 h at 25 °C. When the phase stability of the emulsion was tested over a period of 90 d, the nanoemulsion was found to maintain its integrity in the single liquid phase without phase separation, when formulated using a HCR. The release profiles of niacin emulsion and nanoemulsion formulations were assessed in this study using different methods, such as magnetic stirring, ultrasonic, and hydrodynamic cavitation. The results showed that the nanoemulsion formulations delivered a higher release than the emulsion. Particularly, the nanoemulsion prepared using HCR displayed the highest cumulative release after 12 h. This indicates that the nanoemulsion prepared using hydrodynamic cavitation produced smaller particles than those produced using the other methods. Consequently, it can help deliver the important ingredients in the nanoemulsion formulation into the deeper layer of skin effectively. The analysis of the important parameters of all results for emulsion production using HCR agreed quite well with the requirements of quality for nanoemulsions to be used in skincare products. Therefore, the production of nanoemulsion skincare products using the rotor-stator HCR could be adapted as a very useful and effective process in the cosmetic production industry.

Declaration of Competing Interest

The authors declare that they have no known competing financial interests or personal relationships that could have appeared to influence the work reported in this paper.

Acknowledgement

This project was funded by the Prince of Songkla University (grant no. STS6101021e).

References

[1] R.J. Hay, N.E. Johns, H.C. Williams, I.W. Bolliger, R.P. Dellavalle, D.J. Margolis, R. Marks, L. Naldi, M.A. Weinstock, S.K. Wulf, C. Michaud, C.J.L. Murray, M. Naghavi, The global burden of skin disease in 2010: An analysis of the prevalence and impact of skin conditions, J. Invest. Dermatol. 134 (2014) (2010) 1527–1534, https://doi.org/10.1038/jid.2013.446.
[2] S. Purnamawati, N. Indrastuti, R. Danarti, T. Saefudin, The role of moisturizers in addressing various kinds of dermatitis: A review, Clin. Med. Res. 15 (2017) 75–87, https://doi.org/10.3121/cmr.2017.1363.
[3] M.K. Gupta, S.R. Lipner, Hand hygiene in preventing COVID-19 transmission, J. Am. Acad. Dermatol. 82 (2020) 1215–1216.
[4] D. Schroven, How to reduce skin damage in a COVID-19 world. Dental Nursing, 16 (2020) 612–613, 10.12968/denn.2020.16.12.612.
[5] I. Ahmad, A. Ahmad, S. Iftekhar, S. Khalid, A. Aftab, S.A. Raza, Role of nanoparticle in cosmetics industries, in: Biological Synthesis of Nanoparticles and their Applications, CRC Press, 2020, pp. 173–204.
[6] Global Cosmetic Skin Care Market, Research and markets, The world's largest market research store, (n.d.). https://www.researchandmarkets.com/reports/5141056/cosmetic-skin-care-global-market-trajectory-and (accessed August 4, 2021).
[7] B. Arifin, R. Nasution, S. Savila, R. Ramadani, H. Helwati, M. Marianne, U. Amna, N. Saidi, Sunscreen activities of bark artocarpus heterophyllus against ultraviolet

ray (sun protection factor) in lotion formula, Open Access Maced, J Med. Sci. 8 (2020) 461–467, https://doi.org/10.3889/oamjms.2020.4665.
[8] D.I. Widiputri, S. Wijaya, S.P. Kusumocahyo, Development of skin lotion containing antioxidant extract from coffee pulp and study on its stability, IOP Conf. Ser.: Mater. Sci. Eng. 742 (2020) 012020, 10.1088/1757-899X/742/1/012020.
[9] A.C. Anggelina, D. Pringgenies, E. Yudiati, Potential of sodium alginate in sargassum sp. in lotion preparation to treat incision wound in mice, Int. J. Biol. Educ. 13 (2021) 99–105, 10.15294/biosaintifika.v13i1.22539.
[10] D. Indriati, I.Y. Wiendarlina, A.S. Carolina, Formulation and evaluation of anti-acne lotion containing red ginger (zingiber officinalle roscoe) essential oil, Pharmacol. Clin. Pharm. Res. 3 (2018) 61–65, 10.15416/pcpr.v3i3.19841.
[11] Y.S. Cheng, K.W. Lam, K.M. Ng, R.K.M. Ko, C. Wibowo, An integrative approach to product development–A skin-care cream, Comput. Chem. Eng. 33 (5) (2009) 1097–1113, https://doi.org/10.1016/j.compchemeng.2008.10.010.
[12] M.N. Yukuyama, D.D.M. Ghisleni, T.J.A. Pinto, N.A. Bou-Chacra, Nanoemulsion: Process selection and application in cosmetics – A review, Int. J. Cosmet. Sci. 38 (2015) 13–24, https://doi.org/10.1111/ics.12260.
[13] P. Rajpoot, K. Pathak, V. Bali, Therapeutic applications of nanoemulsion based drug delivery systems: A review of patents in last two decades, Recent Pat. Drug Delivery Formulation. 5 (2011) 163–172, https://doi.org/10.2174/187221111795471427.
[14] R.I. Mahato, A.S. Narang, Pharmaceutical dosage forms and drug delivery, 3rd edition, CRC Press, 2017.
[15] E.A. Tanghetti, L. Stein Gold, J.Q. Del Rosso, T. Lin, A. Angel, R. Pillai, Optimized formulation for topical application of a fixed combination halobetasol/tazarotene lotion using polymeric emulsion technology, J. Dermatol. Treat. 32 (4) (2021) 391–398, https://doi.org/10.1080/09546634.2019.1668907.
[16] L. Jian, Y. Cao, Y. Zou, Dermal-epidermal separation by heat, in: Epidermal Cells, Methods Mol. Biol. (N. Y.) (2019) 23–25, https://doi.org/10.1007/7651_2019_270.
[17] A.S. Kadam, M.P. Ratnaparkhi, S.P. Chaudhary, Transdermal drug delivery: An overview, Int. J. Res. Dev. Pharm. L. Sci. 3 (2014) 1042–1053.
[18] R.P. Selvam, A.K. Singh, T. Sivakumar, Transdermal drug delivery systems for antihypertensive drugs – A review, Int. J. Pharm. Biomed. Res. 1 (2010) 1–8.
[19] Z.A. Aziz, H. Mohd-Nasir, S.H.M. Setapar, W.L. Peng, S.C. Chuo, A. Khatoon, M.N. M. Ibrahim, K. Umar, A. Ahmad, Role of nanotechnology for design and development of cosmeceutical: Application in makeup and skin care, Front. Chem. 7 (2019) 739, https://doi.org/10.3389/fchem.2019.00739.
[20] D.S. Shaker, R.A.H. Ishak, A. Ghoneim, M.A. Elhuoni, Nanoemulsion: A review on mechanisms for the transdermal delivery of hydrophobic and hydrophilic drugs, Sci. Pharm. 87 (2019) 17, https://doi.org/10.3390/scipharm87030017.
[21] A. Gupta, H.B. Eral, T.A. Hattona, P.S. Doyle, Nanoemulsions: Formation, properties and applications, Soft Matter 12 (2016) 2826–2841, https://doi.org/10.1039/C5SM02958A.
[22] S. Manickam, K. Sivakumar, C.H. Pang, Investigations on the generation of oil-in-water (O/W) nanoemulsions through the combination of ultrasound and microchannel, Ultrason. Sonochem. 69 (2020), 105258, https://doi.org/10.1016/j.ultsonch.2020.105258.
[23] M. Sivakumar, S.Y. Tang, K.W. Tan, Cavitation technology–a greener processing technique for the generation of pharmaceutical nanoemulsions, Ultrason. Sonochem. 21 (2014) 2069–2083, https://doi.org/10.1016/j.ultsonch.2014.03.025.
[24] R. Aboofazeli, Nanometric-scaled emulsions (nanoemulsions), Iran, J. Pharm. Res. 9 (2010) 325–326, https://doi.org/10.22037/IJPR.2010.89.
[25] H. Jasmina, O. Džana, E. Alisa, V. Edina, R. Ognjenka, Preparation of nanoemulsions by high-energy and lowenergy emulsification methods, IFMBE Proceedings 62 (2017) 317–322, https://doi.org/10.1007/978-981-10-4166-2_48.
[26] S. Sharma, N. Loach, S. Gupta, L. Mohan, Phyto-nanoemulsion: An emerging nano-insecticidal formulation, Environ. Nanotechnol., Monit. Manage. 14 (2020) 100331, https://doi.org/10.1016/j.enmm.2020.100331.
[27] R.P. Patel, J.R. Joshi, An overview on nanoemulsion: A novel approach, Int. J. Pharm. Sci. Res. 3 (2012) 4640–4650, https://doi.org/10.13040/IJPSR.0975-8232.3(12).4640-50.
[28] S. Yashodamma, G.P. Darshan, R.B. Basavaraj, H.N. Udayabhanu, Ultrasound assisted fabrication of $SrTiO_3$ nanopowders: Effect of electron beam induced structural and luminescence properties for solid state lightning and high temperature dosimetry applications, Opt. Mater. 92 (2019) 386–398, https://doi.org/10.1016/j.optmat.2019.04.030.
[29] M. Venkataravanappa, H. Nagabhushana, B. Daruka Prasad, G.P. Darshan, R. B. Basavaraj, G.R. Vijayakumar, Dual color emitting Eu doped strontium orthosilicate phosphors synthesized by bio-template assisted ultrasound for solid state lightning and display applications, Ultrason. Sonochem. 34 (2017) 803–820, https://doi.org/10.1016/j.ultsonch.2016.07.004.
[30] R. Raviadaran, M.H. Ng, S. Manickam, D. Chandran, Ultrasound-assisted water-in-palm oil nano-emulsion: Influence of polyglycerol polyricinoleate and NaCl on its stability, Ultrason. Sonochem. 52 (2019) 353–363, https://doi.org/10.1016/j.ultsonch.2018.12.012.
[31] S.Y. Tang, P. Shridharan, M. Sivakumar, Impact of process parameters in the generation of novel aspirin nanoemulsions–comparative studies between ultrasound cavitation and microfluidizer, Ultrason. Sonochem. 20 (2013) 485–497, https://doi.org/10.1016/j.ultsonch.2012.04.005.
[32] X. Sun, X. Xuan, Y. Song, X. Jia, L. Ji, S. Zhao, J.Y. Yoon, S. Chen, J. Liu, G. Wang, Experimental and numerical studies on the cavitation in an advanced rotational hydrodynamic cavitation reactor for water treatment, Ultrason. Sonochem. 70 (2021), 105311, https://doi.org/10.1016/j.ultsonch.2020.105311.
[33] Y.M. Oo, G. Prateepchaikul, K. Somnuk, Two-stage continuous production process for fatty acid methyl ester from high FFA crude palm oil using rotor-stator hydrocavitation, Ultrason. Sonochem. 73 (2021), 105529, https://doi.org/10.1016/j.ultsonch.2021.105529.
[34] M. Ashokkumar, R. Rink, S. Shestakov, Hydrodynamic cavitation – an alternative to ultrasonic food processing, Electron. J. Tech. Acoust. 9 (2011).
[35] X. Sun, X. Xuan, L. Ji, S. Chen, J. Liu, S. Zhao, S. Park, J.Y. Yoon, A.S. Om, A novel continuous hydrodynamic cavitation technology for the inactivation of pathogens in milk, Ultrason. Sonochem. 71 (2021), 105382, https://doi.org/10.1016/j.ultsonch.2020.105382.
[36] R. Miller, Emulsifiers: Types and uses, Encycl. Food Health. (2016) 498–502, https://doi.org/10.1016/B978-0-12-384947-2.00249-X.
[37] S. Alam, M.S. Algahtani, M.Z. Ahmad, J. Ahmad, Investigation utilizing the HLB concept for the development of moisturizing cream and lotion: In-vitro characterization and stability evaluation, Cosmetics 7 (2020) 43, https://doi.org/10.3390/cosmetics7020043.
[38] L. Wang, J. Dong, J. Chen, J. Eastoe, X. Li, Design and optimization of a new self-nanoemulsifying drug delivery system, J. Colloid Interface Sci. 330 (2) (2009) 443–448, https://doi.org/10.1016/j.jcis.2008.10.077.
[39] A. Gadhave, Determination of hydrophilic-lipophilic balance value, Int. J. Sci. Res. 3 (2014) 573–575.
[40] S. Leibtag, A. Peshkovsky, Cannabis extract nanoemulsions produced by high-intensity ultrasound: Formulation development and scale-up, J. Drug Delivery Sci. Technol. 60 (2020) 101953, https://doi.org/10.1016/j.jddst.2020.101953.
[41] N. Ng, M.A. Rogers, Surfactants, Encycl. Food Chem. (2019) 276–282, https://doi.org/10.1016/B978-0-08-100596-5.21598-9.
[42] R.F. Rodrigues, I.C. Costa, F.B. Almeida, R.A.S. Cruz, A.M. Ferreira, J.C.E. Vilhena, A.C. Florentino, J.C.T. Carvalho, C.P. Fernandes, Development and characterization of evening primrose (Oenothera biennis) oil nanoemulsions, Rev. Bras. Farmacogn. 25 (4) (2015) 422–425, https://doi.org/10.1016/j.bjp.2015.07.014.
[43] P. Cinelli, M.B. Coltelli, F. Signori, P. Morganti, A. Lazzeri, Cosmetic packaging to save the environment: Future perspectives, Cosmetics 6 (2019) 26, https://doi.org/10.3390/cosmetics6020026.
[44] H. Kim, B. Koo, S. Lee, J.Y. Yoon, Experimental study of cavitation intensity using a novel hydrodynamic cavitation reactor, J. Mech. Sci. Technol. 33 (9) (2019) 4303–4310, https://doi.org/10.1007/s12206-019-0826-8.
[45] Y.M. Oo, G. Prateepchaikul, K. Somnuk, Continuous acid-catalyzed esterification using a 3D printed rotor–stator hydrodynamic cavitation reactor reduces free fatty acid content in mixed crude palm oil, Ultrason. Sonochem. 72 (2021), 105419, https://doi.org/10.1016/j.ultsonch.2020.105419.
[46] A.V. Mahulkar, P.S. Bapat, A.B. Pandit, F.M. Lewis, Steam bubble cavitation, AIChE J. 54 (7) (2008) 1711–1724, https://doi.org/10.1002/aic.11509.
[47] R. van Zwieten, B. Verhaagen, K. Schroën, D. Fernández Rivas, Emulsification in novel ultrasonic cavitation intensifying bag reactors, Ultrason. Sonochem. 36 (2017) 446–453, https://doi.org/10.1016/j.ultsonch.2016.12.004.
[48] M.J. Hidajat, W. Jo, H. Kim, J. Noh, Effective droplet size reduction and excellent stability of limonene nanoemulsion formed by high-pressure homogenizer, Colloids Interfaces. 4 (2020), https://doi.org/10.3390/colloids4010005.
[49] M.M. Narawi, H.I. Chiu, Y.K. Yong, N.N.M. Zain, M.R. Ramachandran, C.L. Tham, S.F. Samsurrijal, V. Lim, Biocompatible nutmeg oil-loaded nanoemulsion as phyto-repellent, Front. Pharmacol. 11 (2020) 214, https://doi.org/10.3389/fphar.2020.00214.
[50] M.R. Abdulbaqi, N.A. Rajab, Apixaban ultrafine O/W nano emulsion transdermal drug delivery system: Formulation, in vitro and ex vivo characterization, Syst. Rev. Pharm. 11 (2020) 82–94.
[51] K.C. Panigrahi, C.N. Patra, M.E.B. Rao, Quality by design enabled development of oral self-nanoemulsifying drug delivery system of a novel calcimimetic cinacalcet HCL using a porous carrier: In vitro and in vivo characterisation, AAPS PharmSciTech 20 (2019) 216, https://doi.org/10.1208/s12249-019-1411-2.
[52] C. Prakash, P. Bhargava, S. Tiwari, B. Majumdar, R.K. Bhargava, Skin surface pH in acne vulgaris: Insights from an observational study and review of the literature, J. Clin. Aesthet. Dermatol. 10 (2017) 33–39.
[53] E. Proksch, pH in nature, humans and skin, J. Dermatol. 45 (9) (2018) 1044–1052, https://doi.org/10.1111/1346-8138.14489.
[54] H. Lambers, S. Piessens, A. Bloem, H. Pronk, P. Finkel, Natural skin surface pH is on average below 5, which is beneficial for its resident flora, Int. J. Cosmet. Sci. 28 (5) (2006) 359–370, https://doi.org/10.1111/j.1467-2494.2006.00344.x.
[55] J. Graf, Considering the pH factor and aging, dermatology, HMP global learning network, (n.d.). https://www.hmpgloballearningnetwork.com/site/thederm/site/cathlab/event/considering-ph-factor-and-aging (accessed June 26, 2021).
[56] A.J. Shnoudeh, I. Hamad, R.W. Abdo, A.Y. L.QadumiiJaber, H.S. Surchi, S. Z. Alkelany, Chapter 15 – Synthesis, characterization, and applications of metal nanoparticles, Biomater. Bionanotechnol. (2019) 527–612, https://doi.org/10.1016/B978-0-12-814427-5.00015-9.
[57] S.D. Costa, M. Basri, N. Shamsudin, H. Basri, Stability of positively charged nanoemulsion formulation containing steroidal drug for effective transdermal application, J. Chem. (2014), https://doi.org/10.1155/2014/748680.
[58] A.S. Zidan, O.A.A. Ahmed, B.M. Aljaeid, Nicotinamide polymeric nanoemulsified systems: A quality-by-design case study for a sustained antimicrobial activity, Int. J. Nanomed. 11 (2016) 1501–1516, https://doi.org/10.2147/IJN.S102945.
[59] S. Peltola, P. Saarinen-Savolainen, J. Kiesvaara, T.M. Suhonen, A. Urtti, Microemulsions for topical delivery of estradiol, Int. J. Pharm. 254 (2) (2003) 99–107, https://doi.org/10.1016/S0378-5173(02)00632-4.

[60] P. Raknam, S. Pinsuwan, T. Amnuaikit, Phenylethyl resorcinol loaded in liposomal cream formulation for cosmeceutical application, J. Pharm. Res. Int. 32 (2020) 64–76, https://doi.org/10.9734/jpri/2020/v32i130396.
[61] L. Binder, J. Mazál, R. Petz, V. Klang, C. Valenta, The role of viscosity on skin penetration from cellulose ether-based hydrogels, Skin Res. Technol. 25 (5) (2019) 725–734, https://doi.org/10.1111/srt.12709.
[62] Chemical book, CAS DataBase List. https://www.chemicalbook.com/CASDetailList_30500_EN.htm (accessed February 25, 2021).
[63] Dow, Safety Data Sheet, Triethanolamine 99%, (n.d.). http://208.112.58.204/pridesol/documents/sds/Triethanolamine%2099%25%20-%20Dow%20-%202015-03-11.pdf (accessed February 26, 2021).
[64] Pub Chem, Nicotinic acid, (n.d.). https://pubchem.ncbi.nlm.nih.gov/compound/Nicotinic-acid (accessed February 26, 2021).
[65] Lubrizol, Carbopol®* Ultrez 21 Polymer, (n.d.). https://www.ge-iic.com/files/fichas%20productos/Carbopol_Ultrez_21_hoja_tecnica.pdf (accessed February 26, 2021).
[66] T. Amnuaikit, T. Phadungkarn, C. Wattanapiromsakul, P. Boonme, Formulation development of antibacterial films containing mangosteen peel extract, Res. J. Pharm. Technol. 5 (2012) 1058–1065.
[67] P. Boonme, N. Suksawad, S. Songkro, Characterization and release kinetics of nicotinamide microemulsion-based gels, J. Cosmet. Sci. 63 (2012) 397–406.
[68] I. Chanda, R. Bordoloi, D.D. Chakraborty, P. Chakraborty, S.R.C. Das, Development and validation of UV-spectroscopic method for estimation of niacin in bulk and pharmaceutical dosage form, J. Appl. Pharm. Sci. 7 (2017) 081–084, https://doi.org/10.7324/JAPS.2017.70911.
[69] S. Dharma, H.H. Masjuki, H.C. Ong, A.H. Sebayang, A.S. Silitonga, F. Kusumo, T.M. I. Mahlia, Optimization of biodiesel production process for mixed jatropha curcas–ceiba pentandra biodiesel using response surface methodology, Energy Convers. Manage. 115 (2016) 178–190, https://doi.org/10.1016/j.enconman.2016.02.034.
[70] E. Bergqvist, T. Tossavainen, M. Johansson, An analysis of high and low intercorrelations between mathematics self-efficacy, anxiety, and achievement variables: A prerequisite for a reliable factor analysis, Educ. Res. Int. (2020), https://doi.org/10.1155/2020/8878607.
[71] S. Chadli, L. Mourad, A. El-Hadj, M. Aissou, F. Boudjema, Impact of Tween 60 on physicochemical properties and stability of pistacia lentiscus fruit oil-in-water emulsion at a semi-low temperature, J. Dispersion Sci. Technol. 40 (2019), https://doi.org/10.1080/01932691.2018.1468266.
[72] L. Basiri, G. Rajabzadeh, A. Bostan, Physicochemical properties and release behavior of Span 60/Tween 60 niosomes as vehicle for α-Tocopherol delivery, LWT-Food, Sci. Technol. 84 (2017) 471–478, https://doi.org/10.1016/j.lwt.2017.06.009.
[73] V.B. Junyaprasert, P. Singhsa, J. Suksiriworapong, D. Chantasart, Physicochemical properties and skin permeation of Span 60/Tween 60 niosomes of ellagic acid, Int. J. Pharm. 423 (2) (2012) 303–311, https://doi.org/10.1016/j.ijpharm.2011.11.032.
[74] X. Guo, J. Yang, Preparation of oleic acid-carboxymethylcellulose sodium composite vesicle and its application in encapsulating nicotinamide, Polym. Int. (2020), https://doi.org/10.1002/pi.6256.
[75] N.Ü. Okur, S. Apaydın, N.Ü.K. Yavaşoğlu, A. Yavaşoğlu, H.Y. Karasulu, Evaluation of skin permeation and anti-inflammatory and analgesic effects of new naproxen microemulsion formulations, Int. J. Pharm. 416 (2011) 136–144, https://doi.org/10.1016/j.ijpharm.2011.06.026.
[76] S.C. Weiss, Conventional topical delivery systems, Dermatol. Ther. 24 (2011) 471–476, https://doi.org/10.1111/j.1529-8019.2012.01458.x.
[77] A.H. Saberi, Y. Fang, D.J. McClements, Fabrication of vitamin E-enriched nanoemulsions: Factors affecting particle size using spontaneous emulsification, J. Colloid Interface Sci. 391 (2013) 95–102, https://doi.org/10.1016/j.jcis.2012.08.069.
[78] R.C. Ribeiro, S.M. Barreto, E.A. Ostrosky, P.A. Rocha-Filho, L.M. Veríssimo, M. Ferrari, Production and characterization of cosmetic nanoemulsions containing opuntia ficus-indica (L.) mill extract as moisturizing agent, Molecules 20 (2015) 2492–2509, https://doi.org/10.3390/molecules20022492.